Fusion Engineering and Design 124 (2017) 183–186

Contents lists available at ScienceDirect

Fusion Engineering and Design

journal homepage: www.elsevier.com/locate/fusengdes

Development and analyses of self-passivating tungsten alloys for DEMO accidental conditions

Tobias Wegener[a,*], Felix Klein[a], Andrey Litnovsky[a], Marcin Rasinski[a], Jens Brinkmann[a,b], Freimut Koch[b], Christian Linsmeier[a]

[a] Forschungszentrum Jülich GmbH, Institut für Energie- und Klimaforschung – Plasmaphysik, Partner of the Trilateral Euregio Cluster (TEC), 52425 Jülich, Germany
[b] Max-Planck-Institut für Plasmaphysik, D-85748 Garching, Germany

HIGHLIGHTS

- Self-passivating W–Cr–Y shows the best oxidation performance of all tested alloys.
- WO_3 formation and evaporation in dry atmosphere is fully mitigated.
- A mechanism which makes oxidation in humid atmospheres so challenging for the W–Cr–Y is introduced and a solution is proposed.

ARTICLE INFO

Article history:
Received 3 October 2016
Received in revised form 10 March 2017
Accepted 14 March 2017
Available online 27 March 2017

Keywords:
Tungsten alloy
Self-passivating tungsten alloy
W–Cr–Y alloy
Humid atmosphere oxidation

ABSTRACT

Tungsten is considered the main candidate material for the first-wall in DEMO due to its high melting point, low erosion yield and low tritium retention. Nevertheless, it can cause a substantial safety issue in a loss-of-coolant accident (LOCA) in combination with air ingress into the plasma vessel, due to the formation and sublimation of volatile neutron activated tungsten oxide. Self-passivating tungsten alloys introduce a passive safety mechanism by forming a stable chromic oxide scale on the surface acting as a diffusion barrier for oxygen and preventing the formation of tungsten oxide. Self-passivating tungsten alloys optimized for oxidation resistance containing ~12 wt.% Cr and ~0.6 wt.% Y are investigated under conditions of argon–oxygen, humid argon and humid air atmospheres at different partial pressures and temperatures ranging from 1073 to 1273 K. Thin films with ~3.5 μm thickness produced by magnetron sputter deposition are used as a model system. The oxidation resistance of these films in an argon–20 vol.% oxygen atmosphere is sufficient to prevent formation and release of tungsten oxide at temperatures of from 1073 to 1273 K. The sublimation of Cr in nitrogen–oxygen–water atmosphere at $T \geq 1273$ K is discussed. A deeper understanding of the governing processes for oxygen/Cr diffusion under different atmospheres is gained, supported by SEM/EDX in combination with FIB cross-section and TGA measurements.

1. Introduction

The conditions in a demonstration fusion reactor like DEMO pose a significant challenge for materials [1]. Accordingly, tungsten (W) is considered the main candidate material for the first wall of a future fusion reactor for its high melting point, low erosion yield, and low tritium retention [2]. Also, in case of a loss-of-coolant accident in combination with air-ingress, W shows a major safety issue. Caused by its linear or catastrophic oxidation behavior, W forms WO_3 which is highly volatile at the predicted temperatures of around 800–1450 K [3]. This could result in the sublimation of several hundred kg h^{-1} of the neutron activated WO_3 [4]. For theses reasons, oxidation of W has to be prevented. In literature typically coatings are applied to prevent W from oxidation in volatilization [5]. However, this is not applicable in a working fusion reactor as all materials facing the plasma are eroded, hence the choice of W due to its low erosion yield. A possible solution for the challenge of oxidation is alloying of W with elements like Cr which form a protective oxide-scale on the surface and so preventing the formation of volatile WO_3 as it was proposed and studied in Refs. [6–11,4]. After the formation of a continuous oxide scale, the diffusion of oxygen through the growing oxide scale becomes the rate

* Corresponding author.
E-mail address: t.wegener@fz-juelich.de (T. Wegener).

http://dx.doi.org/10.1016/j.fusengdes.2017.03.072

Table 1
Oxidation gas mixtures, flow rates, and pressures (p) for the different investigated atmospheres.

Condition	Atmosphere [vol.%]	Flow [ml min^{-1}]	p [Pa]
A	Ar–20O_2	10	10^5
B	Ar–5H_2O	20	10^5
C	N_2–20O_2–5H_2O	20	10^5

determining step [12]. This results in so called parabolic oxidation which can be given as k_p the parabolic oxidation rate. The previous work [4] concentrated on the optimization of the alloy element content resulting to W–∼12 wt.% Cr–∼0.6 wt.% Y and the corresponding samples were only oxidized in dry argon–20 vol.% oxygen (Ar–20 vol.% O_2) atmospheres over short periods of ∼2 h. In this study the W–Cr–Y alloys are further investigated for longer oxidation times of up to 60 h at 1073 K and 9 h at 1273 K both in dry Ar–20 vol.% O_2. Furthermore, oxidation in Ar–5 vol.% H_2O and air–5 vol.% H_2O at 1273 K is investigated to test the actual performance under humid air conditions.

2. Materials and methods of investigations

The samples for this study were produced by magnetron sputtering. The magnetron sputter process was described in [4]. W, chromium (Cr) and yttrium (Y) targets operate simultaneously. For the deposition process titanium (Ti) (99.995 wt.%), Cr (99.95 wt.%), and W (99.95 wt.%) targets were operated by a DC power supply at 100 W for Ti, 180–275 W for Cr and 420–500 W for W. The Y (99.9 wt.%) target was operated with a RF power supply at 140–330 W to achieve reliable deposition rates even at low Y concentrations in the alloys. The alloys were deposited on sapphire substrates, as recommended in Ref. [6]. They have a diameter of 12 mm and 0.5 mm thickness, the deposited films are ∼3.5 μm thick. This was measured using stylus profiler Dektak 6M from Bruker. The composition of the samples is determined separately for each process by wavelength-dispersive X-ray fluorescence (WDXRF) using a sequential X-ray spectrometer (PW2404, PHILIPS). Oxidation testing was performed in a symmetrical double-oven thermogravimetric system (TGA) TAG 16 from Setaram. Furthermore, the system is also equipped with the steam generator. Accordingly, it was possible to perform experiments in Ar–5 vol.% H_2O and air–5 vol.% H_2O. All parameter for the different experiments given in Table 1. Before and after oxidation several analytical techniques like scanning electron microscopy (SEM) in combination with focused ion beam (FIB) cross-sectioning and energy dispersive X-ray spectroscopy (EDX) from Carl Zeiss CrossBeam XB 540, X-ray diffraction (XRD) system from Bruker, were employed to examine the microstructure, homogeneity, elemental composition, and morphology of the alloys and the oxides.

3. Results

3.1. Oxidation in dry atmosphere

In dry Ar–20 vol.% O_2 atmosphere (condition A, Table 1) W shows a fast linear (catastrophic) oxidation behavior forming WO_3, which simultaneously sublimates. Further, the W–Cr alloy shows a parabolic behavior for about 15 min then, fast mass loss is detected. If about 1 wt.% Ti is added to the binary W–Cr the parabolic oxidation behavior is stabilized for up to 30 min. Furthermore, when the Ti is substituted by 0.4–0.7 wt.% Y (Y) the parabolic behavior is stable for up to 2.5 h at 1273 K, followed by a linear weight increase. At 1073 K the parabolic oxidation behavior is increased to more than 60 h (see Table 2 and Fig. 1). In addition, for a film thickness of 7.5 μm this parabolic behavior could even be extended to up to 8.5 h at 1273 K also shown in Fig. 1.

Table 2
Measured parabolic oxidation constants (k_p) (measured with TGA) for different concentrations (WDXRF), temperatures (T) thicknesses (d) (Dektak) in dry Ar–20 vol% O_2 atmosphere condition A (Table 1).

Content [wt.%]	d [μm]	T [K]	Time [h]	k_p [mg^2/cm^4 s]
W–11.1Cr	3.1	1273	0.25	4×10^{-5}
W–10.7Cr–1.1Ti	3.1	1273	0.5	2×10^{-5}
W–11.6Cr–0.4Y	3.5	1273	0.5–2.5	3×10^{-6}
W–13.3Cr–1.1Y	7.5	1273	0.5–8.5	4×10^{-6}
W–13.5Cr–0.7Y	3.5	1073	2–60.0	9×10^{-8}

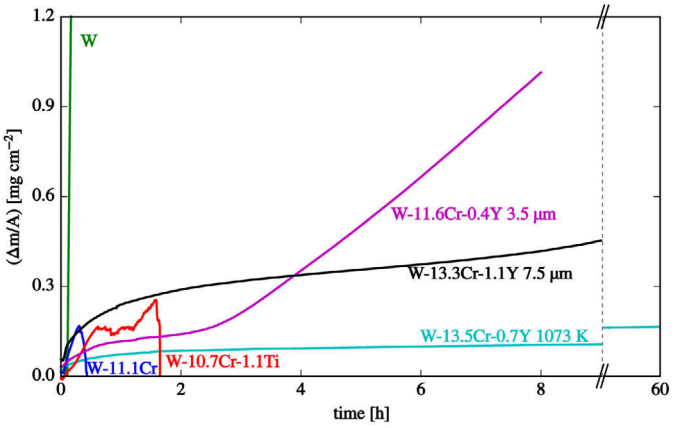

Fig. 1. Oxidation of W, W–Cr, W–Cr–Ti and W–Cr–Y in dry Ar–20 vol.% O_2 atmosphere (condition A, Table 1) at 1273 K.

3.2. Oxidation in humid argon

In humid argon atmosphere condition B (Table 1) W shows a slow linear weight increase in Fig. 2. In fact, slower than all other tested materials under these conditions. W–Cr shows a rather fast but stable parabolic weight increase, the ternary W–Cr–Y on the other hand shows a slower but linear weight gain in Fig. 2.

3.3. Oxidation in humid air

Under the most challenging of all conditions where humidity and oxygen is combined (compare to C, Table 1), W shows an even faster catastrophic oxidation compared to the dry oxygen containing atmosphere case. The short parabolic behavior of W–Cr is further reduced and scale spallation and sublimation occurs.

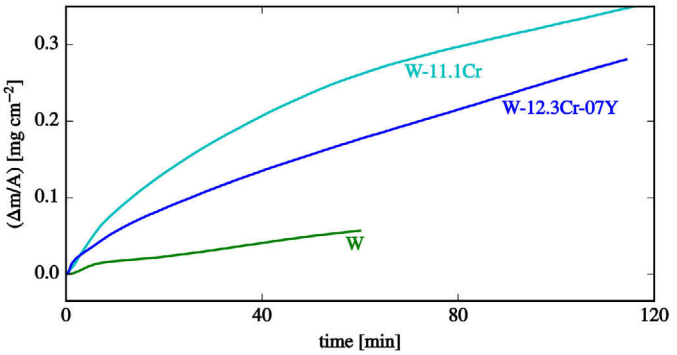

Fig. 2. Oxidation of W, W–Cr, and W–Cr–Y in Ar–5 vol.% H_2O atmosphere (condition B, Table 1) at 1273 K.

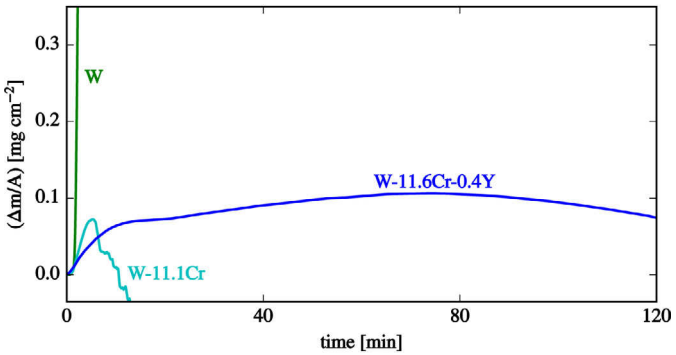

Fig. 3. Oxidation of W, W–Cr, and W–Cr–Y in N_2–20 vol.% O_2–5 vol.% H_2O atmosphere (condition C, Table 1) at 1273 K.

W–Cr–Y shows a very low weight gain with indications for sublimation by ~10 min nearly no weight gain is detectable at the last ~40 min of the curve eve weight loss becomes apparent in Fig. 3.

3.4. Investigation of oxidation and sublimation in H_2O atmospheres

To investigate, which elements are sublimating under the humid air conditions C, thin-film test samples of pure Cr and W were prepared and oxidized under conditions B and C (Table 1). In a first step, the thin films are fully oxidized. Hence, the weight gain of oxidation is not competing with weight loss of sublimation. In the second step, the weight change over time is recorded as shown in Fig. 4. Accordingly, every further weight loss corresponds to sublimation of the species. There is no sublimation detectable for pure Cr in humid Ar atmosphere (B, Table 1), as the weight signal stays constant. However, in humid air (C, Table 1) sublimation is clearly detectable and has a rate of 5×10^{-6} mg cm^{-2} s^{-1}. Furthermore, pure W shows a one order of magnitude higher sublimation rate 7×10^{-5} mg cm^{-2} s^{-1} compared to Cr under the same conditions. To compare the differences in the formed oxide-scales caused by the different atmospheres on the W–Cr–Y alloys, focused ion beam cross-sections were prepared as shown in Fig. 5 with the corresponding oxidation curves on top.

In Fig. 5(a), a 250 ± 30 nm thick and dense protective Cr_2O_3 scale on top is visible, with no indications for WO_3 and just minor internal oxidation in the alloy (dark spots) which was formed under the atmospheric condition A, Table 1. The lighter gray spots in the lower part of the image represent Cr rich (αCr, W) phase which forms at 1273 K similar as the Cr–W phase diagram predicts [13]. This

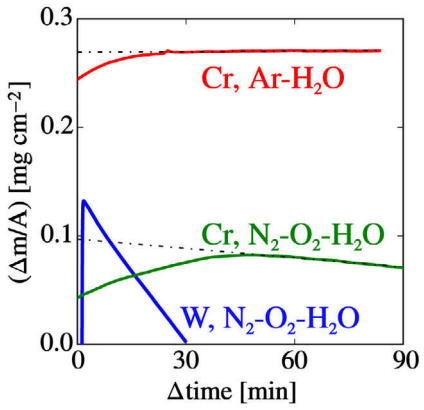

Fig. 4. Weight loss coursed by sublimation after oxidation of pure Cr in Ar–5 vol.% H_2O and N_2–20 vol.% O_2–5 vol.% H_2O (conditions B + C, Table 1) and for pure W in N_2–20 vol.% O_2–5 vol.% H_2O (conditions C, Table 1).

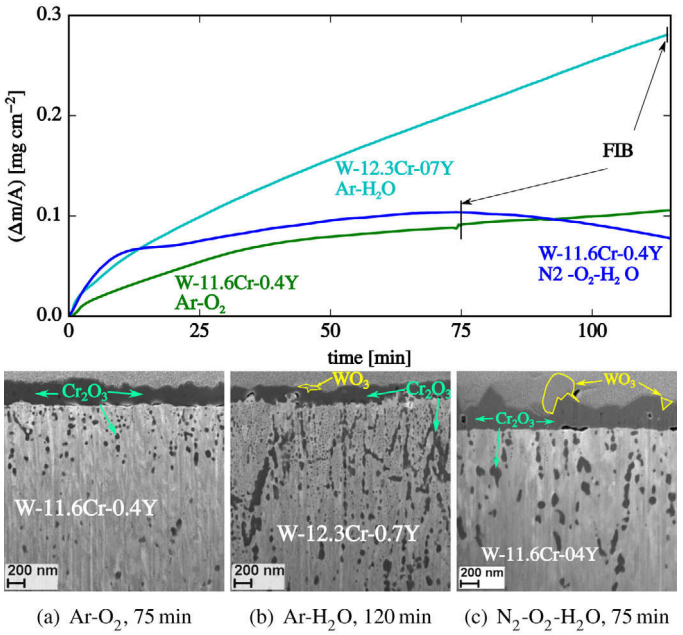

(a) Ar-O_2, 75 min (b) Ar-H_2O, 120 min (c) N_2-O_2-H_2O, 75 min

Fig. 5. Oxidation of W–Cr–Y in different atmospheres at the top, with the corresponding FIB cross-sections of W–Cr–Y thin-film alloys (a) after 75 min oxidation in Ar–20 vol.% O_2 atmosphere (A, Table 1), (b) after 120 min oxidation in Ar–5 vol.% H_2O (B, Table 1), and (c) after 75 min oxidation in (C, Table 1) at 1273 K. (For interpretation of the references to color in this figure citation, the reader is referred to the web version of this article.)

sample corresponds to the 3.5 μm thick W–Cr–Y samples in Fig. 1, for which the oxidation was stopped at 75 min to investigate the favored stable parabolic oxidation behavior.

In Fig. 5(b), vast amounts of internal oxidation are visible, which is dominantly located on the grain boundary and the (α Cr, W) (gray spots), the surface oxide scale is 190 ± 30 nm thick and so ~60 nm thinner than in Fig. 5(a) even though the oxidation time was increased from 75 min to 120 min and weight gain at the point of the FIB-cross section is three times higher. For these reasons, the majority of the weight gain depicted in the curve W–12.3Cr–0.7Y in Fig. 2 is corresponding to internal oxidation in humid argon (B. Table 1). In addition, small amounts of WO_3 are detected on the surface as light spots on the very surface of the oxide marked with yellow.

In Fig. 5(c) an identical period of 75 min was chosen as for the oxidation in dry Ar–20 vol.% O_2 case. The oxidation follows the depicted curve of W–11.6Cr–0.4Y alloy in Fig. 3. The oxide scale on the surface is 280 ± 70 nm similarly thick as for the dry oxidation, but it is to note that also WO_3 was formed at the surface. Furthermore, the internal oxidation is slightly more pronounced than in case of the dry Ar–O_2 oxidation.

4. Discussion

The W–11.6Cr–0.4Y alloy in Fig. 5(a) shows a kind of ideal oxidation behavior as:

1 main mechanism formation of a thick and dense protective Cr_2O_3 scale → parabolic oxidation,
2 no indications for WO_3 formation,
3 minor internal oxidation visible in the cross-section (dark gray spots).

However, after 2.5 h for the 3.5 μm thick W–11.6Cr–0.4Y alloy in Fig. 1 linear oxidation behavior is detected which is correlated to exhaustion of Cr to a content of ~8 wt.%, as discussed in [4]. The

exhaustion of Cr, is followed by formation of WO_3 on the surface (detected by additional EDX measurements), which results in the linear oxidation behavior. This failure, can be delayed by simply increasing the alloy thickness. For example, W–13.3Cr–1.1Y with a thickness of 7.5 μm in Fig. 1 shows an increased parabolic oxidation behavior for 8.5 h.

For Ar–H_2O in Fig. 5(b) the internal oxidation is the dominant process. This could be caused by a different diffusion and adsorption mechanism. As, Cr_2O_3 forms an ionic lattice so the only probable transport is the diffusion of ions through the oxide scale [12]. Further that means, O_2 and H_2O have to first adsorb to the surface to form ions by electron exchange. This is more feasible for the H_2O, as it forms thermodynamically more stable ions by $2H_2O + 2e^- \rightleftarrows H_2 + 2OH^-$ with less charge, distributed on a bigger ion compared to ($O_2 + 4e^- \rightleftarrows 2O^{2-}$) the double charged O^{2-} ion. Altogether, this could lead to a faster adsorption and then diffusion of oxygen, in form of OH^- ions through the Cr_2O_3 scale. Furthermore, the increased amount of hydrogen interstitials originating from ($4Cr + 6OH^- \rightleftarrows 2Cr_2O_3 + 3H_2$) at the metal-oxygen interface combined with low solubility of H_2 in W [2], could expand the W lattice sufficiently so that the diffusivity of oxygen interstitials is increased (as discussed for steels in [14]). This could explain the higher internal oxidation in both humid atmospheres (B and C, Table 1).

For the case of the combination of humidity and oxygen (C, Table 1), the initial partial pressure of oxygen (p_{O_2}) is significantly higher so the formation of Cr_2O_3 is faster. Moreover, the diffusion of the OH^- is added so we see a similar behavior on the surface with a rather thick Cr_2O_3 scale and a increased amount of internal oxidation compared to dry Ar–20 vol.% O_2. The formation of WO_3 could be correlated to the additional increased p_{O_2} at the oxide-metal interface, which would make it possible that also W^{x+} ions form and diffuse to the surface to form WO_3.

5. Summary

Overall, the oxidation in dry atmosphere as depicted in Fig. 1 is very promising and shows for the W–Cr–Y system the favorable parabolic oxidation behavior. The end of this behavior seems to be correlated with the exhaustion of the Cr reservoir as it was already discussed in Ref. [4]. Accordingly, it is shown that the time period of parabolic oxidation could be increased by simply increasing the thickness and thereby the Cr reservoir of the alloy (7.5 μm curve Fig. 1). In addition, for a future fusion reactor like DEMO the first-wall armor thickness is for foreseen to be in the order of ~2 mm [1]. It seems probable that this thickness would be sufficient to stay in the parabolic oxidation behavior for a full period of a loss-of-coolant accident.

However, the performance of the W–Cr–Y in humid atmosphere has to be improved drastically as sublimation of neutron activated Cr and especially the ten times higher sublimation of W has to be prevented under all circumstances. One way to improve the situation, at least for Cr is to alloy small amounts of manganese (Mn), as it is done for alloys directly developed to reduce the Cr sublimation [14]. This and the production of bulk test alloys will be subject in future studies.

Acknowledgements

The authors want to acknowledge support by Alexis Terra with the magnetron sputter device. This work has been carried out within the framework of the EUROfusion Consortium and has received funding from the Euratom research and training programme 2014–2018 under grant agreement no. 633053. The views and opinions expressed herein do not necessarily reflect those of the European Commission.

References

[1] Y. Igitkhanov, B. Bazylev, I. Landman, R. Fetzer, Design Strategy for the PFC in DEMO Reactor, KIT SCIENTIFIC REPORTS (Report-Nr. KIT-SR 7637), 2013.
[2] H. Bolt, V. Barabash, G. Federici, J. Linke, A. Loarte, J. Roth, K. Sato, Plasma facing and high heat flux materials – needs for ITER and beyond, J. Nucl. Mater. 307–311 (Part 1) (2002) 43–52, http://dx.doi.org/10.1016/S0022-3115(02)01175-3.
[3] D. Maisonnier, P.I. Cook, R.A. Sardain, L.D. Pace, R. Forrest, L. Giancarli, S. Hermsmeyer, P. Norajitra, N. Taylor, D. Ward, A Conceptual Study of Commercial Fusion Power Plants, Final Report of the European Fusion Power Plant Conceptual Study (PPCS) EFDA(05)-27/4.10, EFDA, 2005.
[4] T. Wegener, F. Klein, A. Litnovsky, M. Rasinski, J. Brinkmann, F. Koch, C. Linsmeier, Development of yttrium-containing self-passivating tungsten alloys for future fusion power plants, Nucl. Mater. Energy 9 (2016) 394–398, http://dx.doi.org/10.1016/j.nme.2016.07.011 www.sciencedirect.com/science/article/pii/S235217911530123X.
[5] H.J. Nolting, R.A. Jefferys, Oxidation Resistant High Temperature Protective Coatings for Tungsten, Tech. Re ML-TDR-6A-227, Air Force Materials Laboratory Research and Technical Division Air Force Systems Command Wright-Patterson Air Force Base, Ohio, 1964 www.dtic.mil/cgi-bin/GetTRDoc?Location=U2&doc=GetTRDoc.pdf&AD=AD0608510.
[6] F. Koch, S. Koeppl, H. Bolt, Self passivating W-based alloys as plasma-facing material, J. Nucl. Mater. 386-388 (2009) 572–574, http://dx.doi.org/10.1016/j.jnucmat.2008.12.179, Materials Proceedings of the Thirteenth International.
[7] T. Weissgaerber, B. Kloeden, B. Kieback, Self-passivating tungsten alloys, Powder Metall. World Congr. Exhibit. 3 (2010) 377–383, iSBN: 978-1-899072-12-5.
[8] F. Koch, J. Brinkmann, S. Lindig, T.P. Mishra, C. Linsmeier, Oxidation behaviour of silicon-free tungsten alloys for use as the first wall material, Phys. Scr. (T145) (2011) 014019 http://stacks.iop.org/1402-4896/2011/i=T145/a=014019.
[9] S. Telu, A. Patra, M. Sankaranarayana, R. Mitra, S. Pabi, Microstructure and cyclic oxidation behavior of W-Cr alloys prepared by sintering of mechanically alloyed nanocrystalline powders, Int. J. Refract. Metals Hard Mater. 36 (0) (2013) 191–203, http://dx.doi.org/10.1016/j.ijrmhm.2012.08.015.
[10] S. Telu, R. Mitra, S.K. Pabi, Effect of Y_2O_3 addition on oxidation behavior of W–Cr alloys, Metall. Mater. Trans. A 46 (12) (2015) 5909–5919, http://dx.doi.org/10.1007/s11661-015-3166-z.
[11] A. Calvo, N. Ordás, I. Iturriza, F. Koch, H. Greuner, G. Pintsuk, C. Sarbu, C. García-Rosales, Manufacturing and testing of self-passivating tungsten alloys of different composition, Nucl. Mater. Energy (2015).
[12] N. Birks, G. Meier, F. Pettit, Introduction to the High-Temperature Oxidation of Metals, Cambridge University Press, 2006.
[13] L. Kaufman, H. Nesor, Calculation of superalloy phase diagrams: Part IV, Metall. Trans. A 6 (11) (1975) 2123–2131, http://dx.doi.org/10.1007/BF03161839.
[14] W.J. Quadakkers, J. Zurek, Oxidation in steam and steam/hydrogen environments, Shreir's Corros. 1 (2010) 407–456.